Cherenkov Photon Background for Low-Noise Silicon Detectors in Space

Manuel E. Gaido [1, 2], Javier Tiffenberg [2], Alex Drlica-Wagner [2, 3], Guillermo Fernández Moroni [2], Bernard J. Rauscher [4], Fernando Chierche [5], Darío Rodrigues [1], Lucas Giardino [1], Juan Estrada [2]

[1] Universidad de Buenos Aires, [2] Fermilab, [3] University of Chicago, [4] NASA Goddard, [5] Universidad Nacional del Sur

FERMILAB-POSTER-24-0075-LDRD-PPD

Introduction

Future space observatories dedicated to the direct imaging and spectroscopy of extra-solar planets require ultra-low-noise detectors sensitive at ultraviolet (UV) to infrared (IR) wavelengths [1,2]. When observing faint sources, detector noise must be studied and minimized in order to maximize signal-to-noise (SNR). However, due to the intense radiation environment of space and the demonstrated ultra-low-noise achievable by modern detectors, Cherenkov radiation emerges as a relatively unexplored source of low-energy background [3].

Cherenkov photon production

The Cherenkov effect [3] is the process by which a charged particle emits electromagnetic radiation when crossing a polarizable material (Fig. 1). In order for this to happen, the particle must have a speed greater to the phase velocity of light in the medium (dependant on photon frequency). For silicon, this means that photon emission drops sharply above ~4eV [4,5]. This results primarily in single-electron events (SEE), which can be significantly spatially separated from the track of the high energy primary [6].

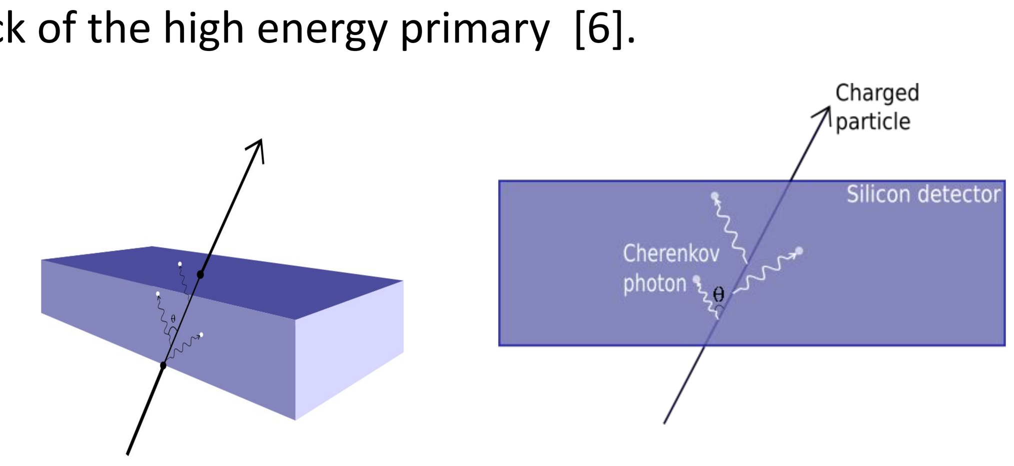

Fig 1: Charged particle crossing silicon and radiating Cherenkov photons that are absorbed in the silicon bulk as single-electron events (SEE).

Model and Validation with Real Data

We construct high-precision simulations that combine GEANT4 particle-matter interactions [7] with a model for Cherenkov radiation in a dielectric medium. Using a dataset of ultra-low-noise images taken with a Skipper CCD at surface level [8], we validate our Cherenkov radiation model for silicon detectors. Filtering for atmospheric muon tracks, we characterized the low-energy halo of SEE around these tracks and show good agreement with our models (Fig. 2).

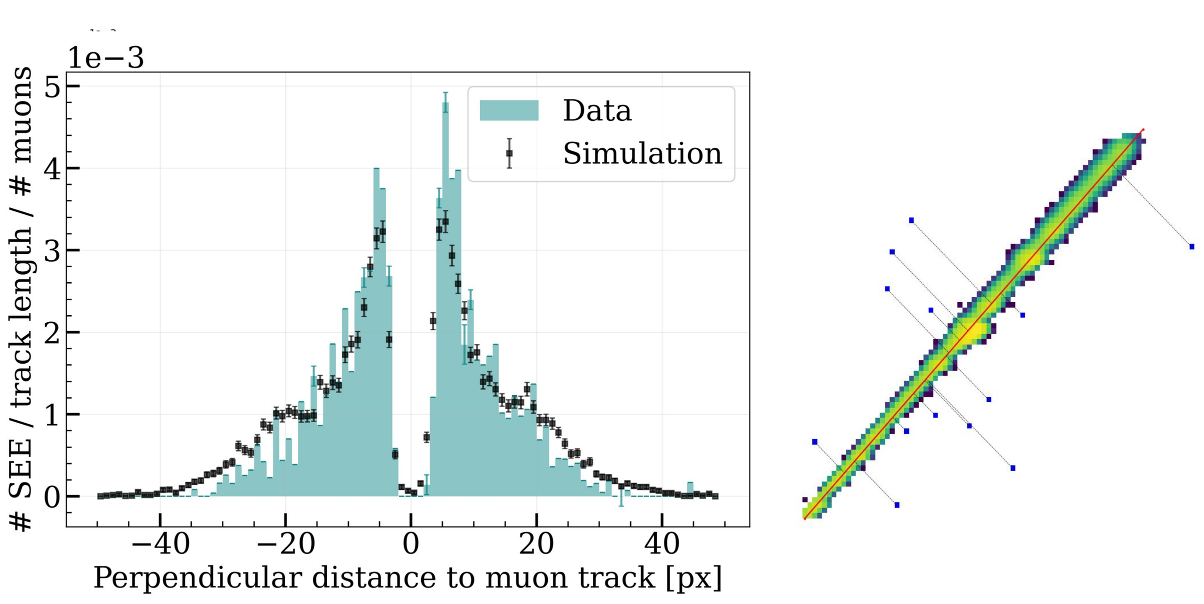

Fig 2: (Left) Example muon track, with best-fit line to which Cherenkov photon distances are computed. (Right) Distribution of distances between muon track and SEE for data (teal histogram) and model (black points).

Simulation of Space Environment

The cosmic-ray environment in low-earth orbit (LEO) and at the L2 Lagrange point consists primarily of protons with a steeply falling energy spectrum [9]. We have simulated this environment for a 250 µm-thick silicon detector with a geometry of 2k x 2k, 15 µm pixels (Fig. 3). This detector thickness is characteristic of Skipper CCDs that provides high quantum efficiency at near-infrared wavelengths [10].

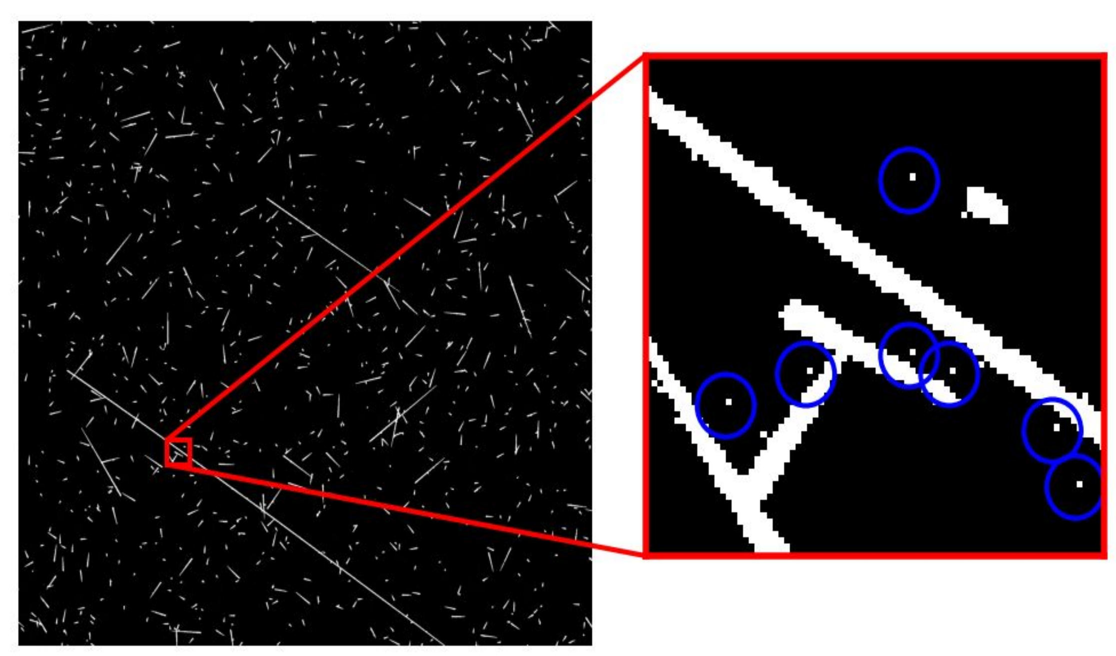

Fig 3: Simulated 30s exposure for a 2k x 2k, 15µm pixel, 250 µm thick silicon detector in LEO including cosmic-ray proton tracks and secondary Chernenkov photons. The expected proton rate is ~950 particles per image, each of which has some probability of generating one or more Cherenkov photons (inset; blue circles).

For image processing, we set an energy threshold of 25e- to identify cosmic-ray tracks. We then dilate these high energy tracks outwards a fixed distance ("masking radius"). The masked area of each image is removed when combining exposures to increase exposure time. The SEE that were not removed by the masking make up the Cherenkov background rate. A bigger masking radius means a smaller effective exposure time per pixel, but reduces the background rate in return (Fig. 4 and 5).

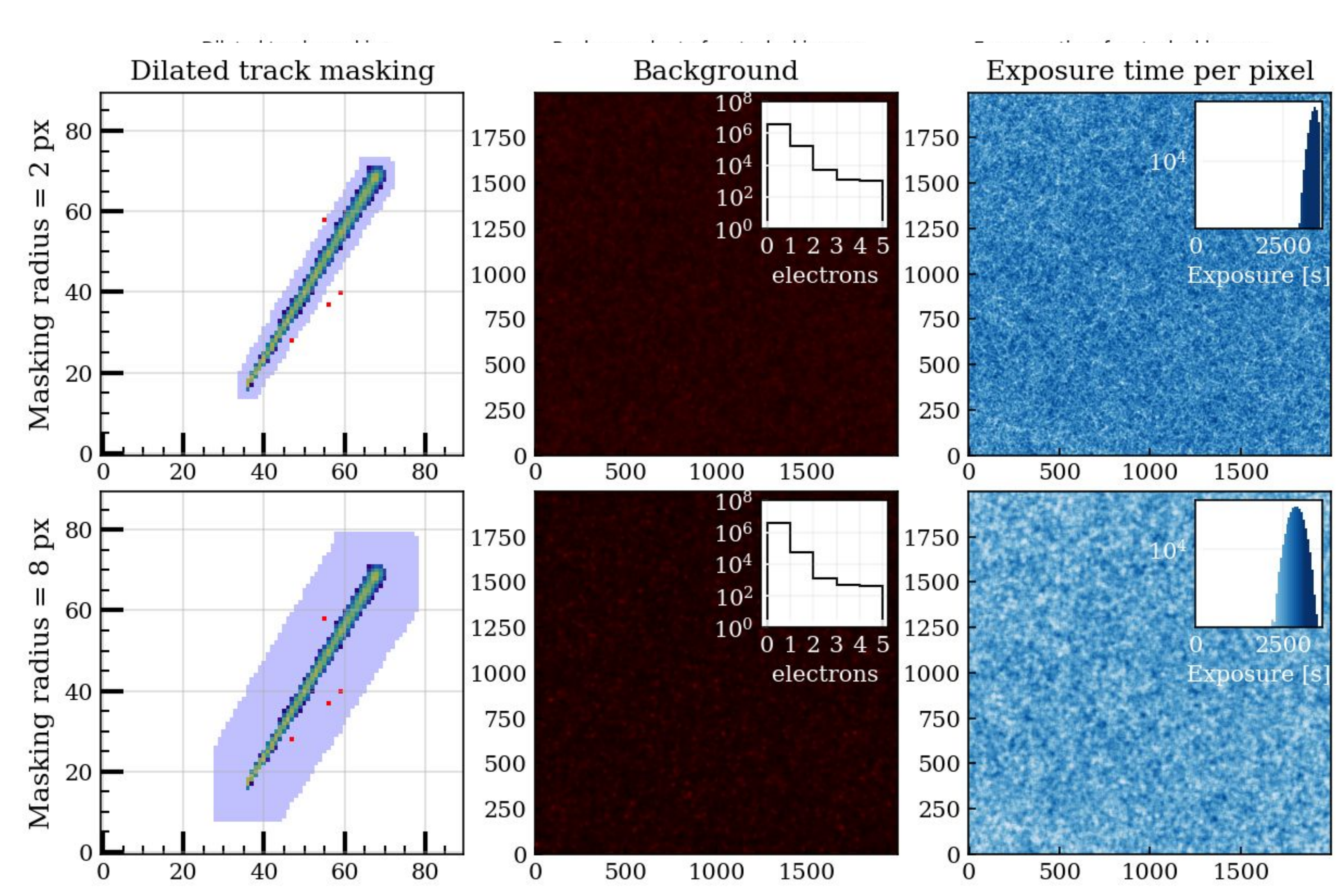

Fig 4: (Left) Examples of small (2 pixel; top) and large (8 pixel; bottom) masking radii around a simulated proton track and secondary Cherenkov photons. (Middle) Simulated residual Cherenkov photon rate after masking and combining 120x30s exposures. (Right) Effective exposure time for 120x30s exposures after masking.

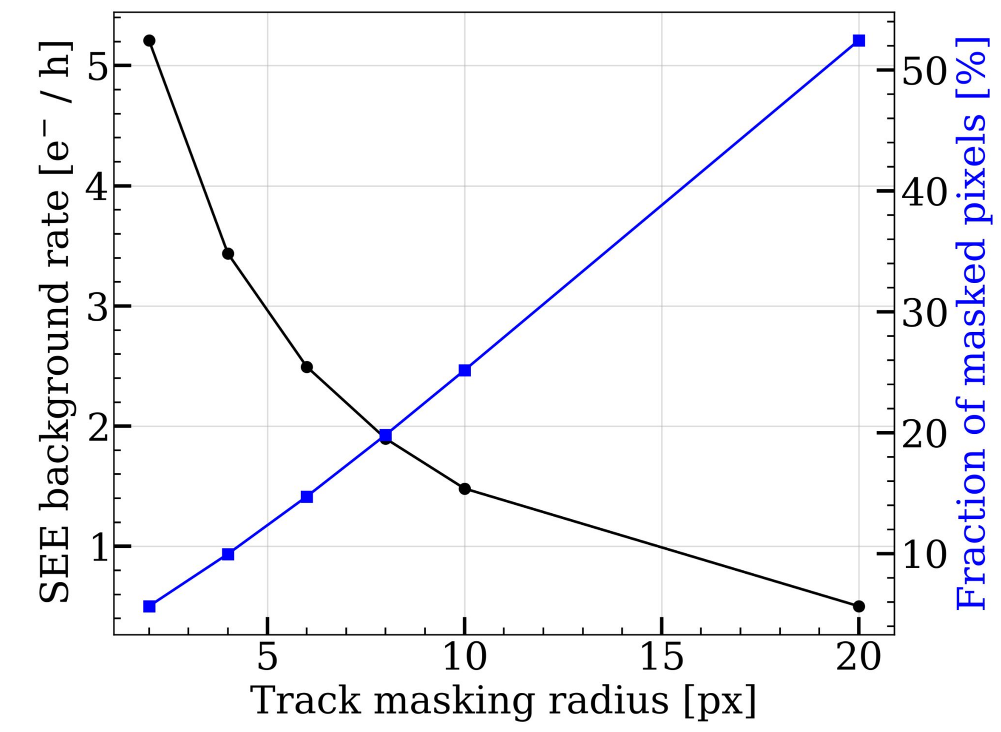

Fig 5: Residual Cherenkov background rate and fraction of masked pixels as a function of the masking radius for a 2k x 2k detector after a 30s exposure. A higher fraction of masked pixels translates into a lower effective exposure time.

Results

The Cherenkov background rate is in the order of ~1e-/h for range of 2-20px of masking radii. We compare this rate to other sources of background in Skipper CCDs. These sources of background, including readout noise and dark current (intrinsic) and speckle and zodiacal light (extrinsic) [11], are of the same magnitude as the Cherenkov background rate (Fig. 6). We emphasize that the Cherenkov background is an irreducible background in silicon detectors. Thinner detectors will have a lower rate, but will also be less sensitive to near-infrared photons.

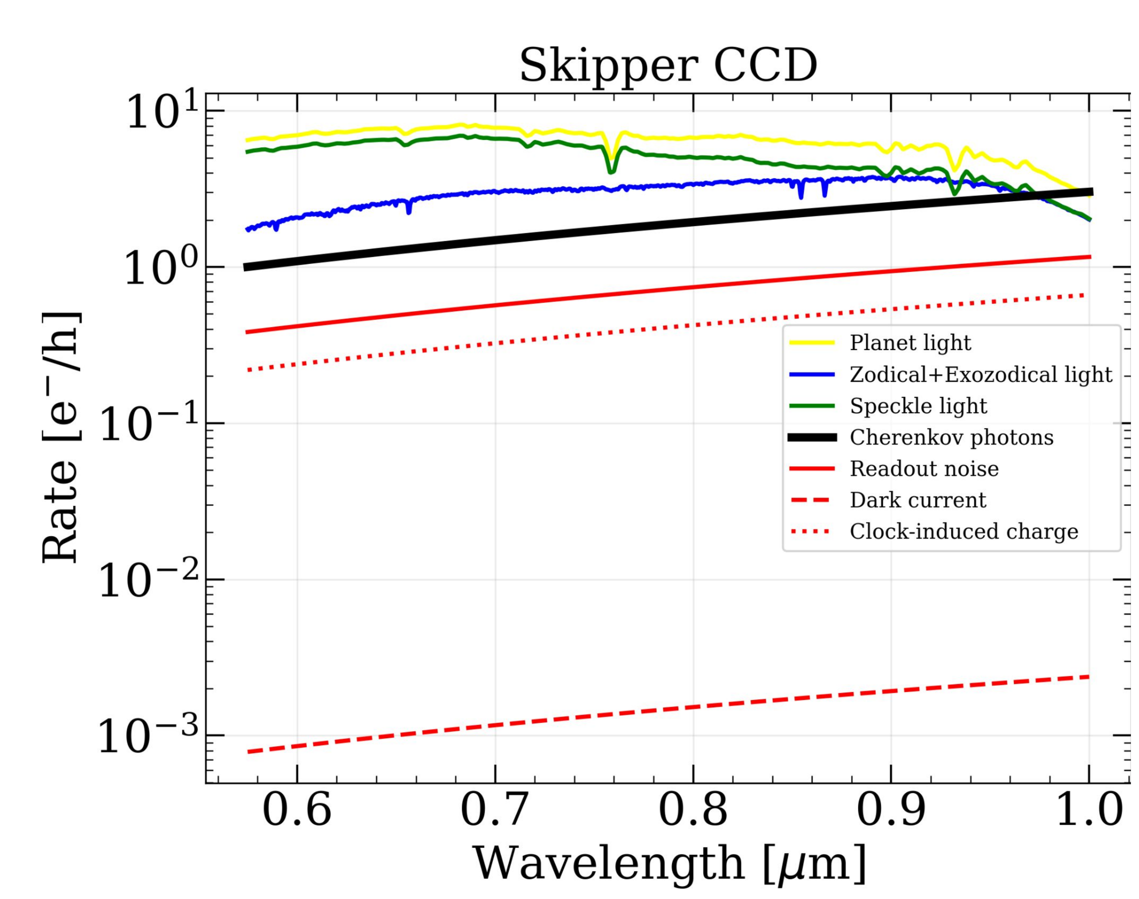

Fig 6: Signal and background sources for exo-planet spectroscopy using a Skipper CCD as a function of wavelength. This figure was generated for a realization of the Roman-CGI in IFS mode observing a 5.0 mag G0V primary and a Jupiter-radius planet orbiting at a separation of 3.8 AU observed at a distance of 10 pc using software provided by [11].

References

1. B. Crill & N. Siegler *Space Technology for Directly Imaging and Characterizing Exo-Earths,* Proc. SPIE. 10398, (2017)
2. *Pathways to Discovery in Astronomy and Astrophysics for the 2020s,* NASEM *(2021)*
3. P. A. Čerenkov, *Visible light from clear liquids under the action of gamma radiation,* C. R. Acad. Sci. USSR 8, 451 (1934)
4. P. Du, R. Essig, et. al, *Sources of Low-Energy Events in Low-Threshold Dark Matter and Neutrino Detectors*, PRX 12, 011009 (2022)
5. M. A. Green, *Self-consistent optical parameters of intrinsic silicon at 300 K including temperature coefficients,* Sol. Energy Mater. Sol. Cells 92, 11 (2008)
6. K. Ramanathan & N. Kurinsky, *Ionization Yield in Silicon for eV-Scale Electron-Recoil Processes*, PRD 102, 063026 (2020)
7. S. Agostinelli et al. *Geant4—a simulation toolkit,* NIMA 506, 3 (2003)
8. Giardino, et. al., *Low energy depositions using smart electronic readout on Skipper-CCD for lightweight Dark Matter experiment,* Argentine Conference on Electronics (2020)
9. Particle Data Group, *Review of Particle Physics*
10. E. Marrufo Villalpando et al. *Characterization and Optimization of Skipper CCDs for the SOAR Integral Field Spectrograph,* PASP 136 045001 (2024)
11. B. Lacy, et al., *Characterization of Exoplanet Atmospheres with the Optical Coronagraph on WFIRST*, AJ, 157, 132 (2019)

Acknowledgements

This work was partially funded by Fermilab LDRD (2019.011, 2022.054), NASA APRA (No. 80NSSC22K1411), and the Heising-Simons Foundation (#2023-4611). This manuscript has been authored by Fermi Research Alliance, LLC under Contract No. DE-AC02-07CH11359 with the U.S. Department of Energy, Office of Science, Office of High Energy Physics. The United States Government retains and the publisher, by accepting the article for publication, acknowledges that the United States Government retains a non-exclusive, paid-up, irrevocable, world-wide license to publish or reproduce the published form of this manuscript, or allow others to do so, for United States Government purposes.

Contact

- Manuel Gaido: manu.gaido@gmail.com
- Javier Tiffenberg: javiert@fnal.gov
- Alex Drlica-Wagner: kadrlica@fnal.gov